THE JOURNAL OF PHYSICAL CHEMISTRY A

Article

pubs.acs.org/JPCA

Multipass Millimeter/Submillimeter Spectrometer to Probe Dissociative Reaction Dynamics

Jacob C. Laas, Brian M. Hays, and Susanna L. Widicus Weaver*

Department of Chemistry, Emory University, Atlanta, Georgia 30322, United States

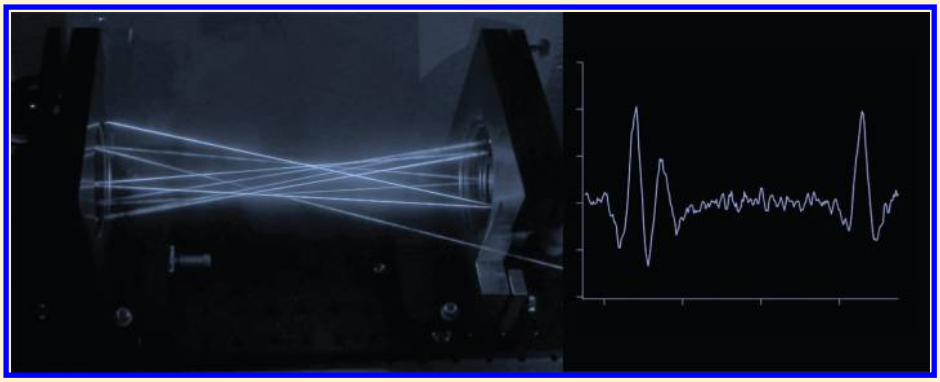

ABSTRACT: We present here the instrument design and first experimental results from a multipass millimeter/submillimeter spectrometer designed to probe dissociative reaction dynamics. This work focuses on benchmarking the instrument performance through detection of the CH_3O and H_2CO products from methanol dissociation induced by a high-voltage plasma discharge. Multiple rotational lines from CH_3O and H_2CO were observed when this plasma discharge was applied to a sample of methanol vapor seeded in an argon supersonic expansion. The rotational temperature of the dissociation products and their abundance with respect to methanol were determined using a Boltzmann analysis. The minimum detectable absorption coefficient for this instrument was determined to be $\alpha_{min} \leq 5 \times 10^{-9}$ cm^{-1}. We discuss these results in the context of future applications of this instrument to the study of photodissociation branching ratios for small organic molecules that are important in complex interstellar chemistry.

INTRODUCTION

Spectroscopic and mass spectrometric techniques are widely used for state-selective measurements on molecular reactants and products during dissociation reactions.[1] Such studies are critically important to the field of astrochemistry, where the dissociative reaction dynamics of small organic molecules dictate the formation of key reaction intermediates such as organic radicals and ions. These small reactive species are the drivers of organic chemistry in interstellar environments through both condensed-phase chemistry on ice surfaces in dense molecular clouds, and gas-phase chemistry in star- and planet-forming regions.[2] Therefore, a full quantitative understanding of radical and ion formation, including product energies and branching ratios, is required to guide accurate astrochemical modeling of these interstellar environments. Surprisingly, while rotationally resolved spectroscopic methods are often used in reaction dynamics studies,[1] very few experiments utilize pure rotational spectroscopic techniques. A few reaction dynamics studies of organic molecules have been conducted using microwave and millimeter spectrometers,[3−5] but to our knowledge, no reaction dynamics studies have yet utilized rotational spectroscopy at higher frequencies within the THz spectral range.

The THz spectral range, also known as the far-infrared (FIR) or submillimeter region, lies between the microwave and infrared spectral windows and includes frequencies from 100 GHz to 10 THz (3−300 cm^{-1}). Rich molecular information can be accessed by THz studies, including the pure rotational signatures of small molecules, the low-frequency vibrational modes of large molecules, and the complex spectral signatures associated with molecular internal motion. The present work focuses on the application of THz spectroscopy to high-resolution pure rotational spectroscopy. THz spectroscopy offers a unique opportunity for the study of chemical mechanisms like the dissociation reactions of small organics because it probes structure-specific spectral fingerprints, enabling the direct detection of reactive species. The structure specificity of rotational spectroscopy is particularly valuable for the study of organic molecules, where dissociation mechanisms may involve many separate channels in which products have either overlapping spectral signatures in other wavelength ranges, or equal masses that preclude mass spectrometry

Special Issue: Oka Festschrift: Celebrating 45 Years of Astrochemistry

Received: December 12, 2012
Revised: May 3, 2013
Published: May 16, 2013

   dx.doi.org/10.1021/jp3122402 | J. Phys. Chem. A 2013, 117, 9548−9554

studies. Any dissociation product that has a permanent dipole moment can be probed using rotational spectroscopy.

The gas-phase spectroscopic study of reactive species as is required in dissociative reaction dynamics studies necessitates the use of a supersonic expansion source combined with a suitable production technique for the molecule of interest, i.e., dissociation of a precursor molecule using a UV lamp, laser, or high-voltage plasma discharge. At sufficiently low sample concentration relative to the inert carrier gas, the supersonic expansion can be used to both quench the excess energy of the dissociation products and to reduce recombination reactions, thus enabling the spectroscopic interrogation of products while minimizing additional complications from excited vibrational states and further reactions.

The use of such sources complicates THz spectroscopy experiments. While the adiabatic cooling offered by supersonic expansions yields an increase in line intensities due to a reduction in the molecular partition function, the path length through the sample is significantly reduced when compared to the long path length direct absorption techniques commonly used in this frequency range. The already weak signals from trace amounts of sample combined with this shortened path length limit the application of this approach for reaction dynamics studies. Standard direct absorption spectrometers that operate in the millimeter/submillimeter range have detection limits on the order of $\sim 10^{-6}$ (see the review by De Lucia[6] and references therein). This is the best case scenario for an experiment involving a supersonic expansion, where the path length through the sample is significantly shortened over the more common long path length direct absorption spectrometers. This detection limit cannot rival the common parts per billion or better detection limits offered by techniques such as laser-induced fluoroescence and mass spectrometry. Therefore, advancements in pure rotational studies as applied to reaction dynamics rely upon increasing the sensitivity of THz spectrometers. There have been a few efforts to extend cavity-enhanced spectral techniques into this frequency range,[7−9] but implementation is challenging because of limitations in appropriate hardware. For example, the new THz chirped-pulse Fourier Transform technique[10] offers detection limits on the order of 10^{-9}, which corresponds to a minimum detectable absorption coefficient, $(\alpha_{min}) \sim 4 \times 10^{-9}$ cm^{-1}. However, the technology upon which this technique is based is either prohibitively expensive for most applications or not yet widely available.

A straightforward method for increasing spectral sensitivity is to increase the optical path length through the sample using an optical arrangement that provides multiple passes while minimizing optical loss factors. To this end, we have adopted the optical design of Perry and co-workers[11] used at visible/infrared wavelengths, which was specifically designed for application to molecular beams due to its minimally sized interaction region. A similar optical design has been used for THz spectroscopy[12] at much higher frequencies (>1.8 THz), but this range is better-suited for studies of rovibrational transitions and torsional states of larger molecules. We have therefore extended this design into the millimeter and submillimeter wavelength ranges, which enables rotational studies of a variety of polyatomic organic molecules that have strong spectral signatures at frequencies in the 100 GHz to 1 THz range. We have coupled this spectrometer with a high-voltage plasma discharge supersonic expansion source to search for methanol dissociation products.

Here, we report the instrument design for this multipass millimeter/submillimeter spectrometer; we also present the first experimental results from this instrument, which involve the detection of methanol dissociation products. The work presented herein is a proof-of-concept study to verify that the spectral technique is of sufficient sensitivity to quantify highly reactive dissociation products. We describe the implications of these findings for future studies of photodissociation mechanisms in the context of interstellar chemistry. Lastly, we discuss other techniques that could be used in conjunction with this experimental technique to provide a more complete understanding of dissociative reaction dynamics.

BACKGROUND

Our reaction dynamics experiments rely on the structure-specificity of THz spectroscopic measurements. Therefore, the critical first step in any such study is to obtain a general overview of the chemistry involved in the reaction mechanism, so that the necessary structural information for each target molecule can be sought to guide the laboratory investigations. We summarize here the available information concerning the methanol dissociation mechanism that pertains to a rotational spectroscopic study.

Several theoretical studies of methanol dissociation have determined the stationary points and transition states for the pathways involved in the dissociation mechanism.[13−16] The following reaction pathways have been considered for methanol decomposition:

$$CH_3OH \rightarrow CH_2OH + H \quad (1a)$$

$$\rightarrow CH_3O + H \quad (1b)$$

$$\rightarrow CH_2 + H_2O \quad (1c)$$

$$\rightarrow CH_3 + OH \quad (1d)$$

$$\rightarrow H_2CO + H_2 \quad (1e)$$

$$\rightarrow HCOH + H_2 \quad (1f)$$

Dissociation channels 1a−1f are all shown to be energetically accessible within a range of ∼30 kcal/mol.[15,16] It is therefore likely that all of these channels play a role in the experiments presented here. Traditional mass spectrometric techniques prove difficult for a methanol dissociation study because neither the CH_2OH versus CH_3O channels nor the CHOH versus H_2CO channels can be distinguished. However all of these product channels have strong THz spectral signatures. The pure rotational spectrum of the CH_3O radical has been characterized up to 400 GHz.[17,18] The H_2CO rotational spectrum has been characterized up to 2.6 THz.[19,20] The OH rotational spectrum has been characterized up to 4 THz,[21−24] but the rotational lines that fall within the range of our spectrometer are too weak to be detected by these methods. No rotational spectrum is available for CHOH, and only infrared spectroscopic data are available for CH_2OH.[25] Because of the limited availability of rotational spectra for all channels, our initial experiments have focused on the CH_3O and H_2CO products.

This work is motivated by the desire to study the photodissociation dynamics of organic molecules that drive complex interstellar chemistry. Methanol photodissociation is an important process in interstellar chemistry, as it is thought to be the dominant mechanism driving a complex network of

dx.doi.org/10.1021/jp3122402 | J. Phys. Chem. A 2013, 117, 9548−9554

organic chemistry in interstellar ices. Specifically, methanol photodissociation provides the radical precursors for the formation of the structural isomers methyl formate, glycolaldehyde, and acetic acid in star-forming regions.[2,26] The branching ratios for methanol photodissociation are therefore crucial parameters needed to guide astrochemical models. Some estimates of the methanol photodissociation branching ratios from experiments on interstellar ice analogues do exist.[27] However, no complete studies of methanol dissociation pathways have been conducted under conditions relevant to astrochemistry in the condensed or gas phase. It should be noted that there have been a number of gas-phase laboratory studies of methanol photodissociation.[28−36] However, none of these studies have clearly distinguished between the CH_2OH and CH_3O channels while also determining quantitative branching ratios. It is generally agreed that either the CH_2OH or CH_3O channel dominates in methanol dissociation reactions. Given the uncertainties in this mechanism and the novel approach of applying rotational spectroscopy to this problem, in the current study we sought to lay the groundwork for future methanol photodissociation studies by first examining the detectability of the methanol dissociation products given in eqs 1a−1f.

EXPERIMENTAL METHODS

Our initial studies have applied multipass millimeter/submillimeter direct absorption spectroscopy to the investigation of the methanol dissociation mechanism. A schematic diagram of this setup is shown in Figure 1. Methanol (Fisher Scientific, Certified ACS solvent grade, 99.9%) was diluted to ∼1% in argon carrier gas (NexAir, ultrahigh purity) by bubbling the carrier gas through the liquid methanol sample at room temperature and then diluting this mixture with additional argon. A pulsed valve (Parker Hannifin, Series 9) introduced the methanol/argon mixture into a vacuum chamber through a 1 mm pinhole nozzle; a nozzle backing pressure of 0.5−1 atm was used. The plasma discharge source that was attached to the front of the pulsed valve is described in more detail below. After dissociation, the gas mixture was expanded adiabatically into the chamber. The pulsed nozzle was set to a repetition rate of 18 Hz with an on-duration of 5 ms. A combined rotary vane + roots blower pumping system with an effective pumping speed at the valve of ∼250 L s^{-1} was used to maintain a chamber pressure of 30 ± 5 mTorr. These operating conditions were found to give the best compromise between signal strength and sample cooling.

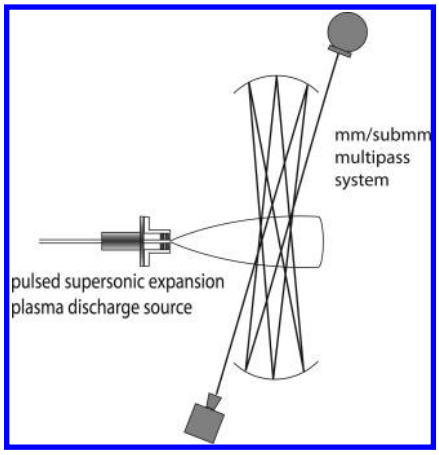

Figure 1. Schematic of the multipass spectrometer coupled with the supersonic expansion discharge source.

The millimeter/submillimeter signal was generated by multiplication of the output signal from an analog signal generator (Agilent Technologies, E8257D PSG with the options 1EA, UNU, 550, and UNT). The output signal was frequency modulated at 15 kHz and then multiplied to the appropriate frequency range using a custom-built frequency multiplier extender kit (Virginia Diodes, Inc.). This multiplier chain has several sets of multipliers and power amplifiers, enabling full frequency coverage from 50−1000 GHz. The specific components used in the experiments described here included a K_a-Band power amplifier (A-2050, Marki Microwave) plus a WR8 × 3 tripler (Virginia Diodes, Inc.) to provide a nominal output frequency range of 90−140 GHz. The output range of this multiplier was often extended during these experiments to higher frequencies (∼145 GHz) where sufficient output power is available. The output radiation from the multiplier was coupled into the multipass optical setup using a standard waveguide horn. The THz radiation was aligned in the multipass arrangement described by Kaur et al.; spherical mirrors having a 7.62 cm diameter and focal length (Edmund Optics, NT32-824) and spaced at a distance of 28.5 cm were used to produce 7 optical passes in the vacuum chamber. The number of passes was limited by the power lost (∼90%) from clipping the large beam at the edges of the spherical mirrors. The beam waist region of the optical path crossed the center of the expansion ∼2.5 cm downstream from the dissociation region, oriented such that the optical path was parallel to the benchtop and in-plane with the centerline of the gas expansion. This orientation ensured that all optical passes crossed the molecular beam in the coldest part of the expansion. The output signal from the multipass cavity was monitored with a zero-bias diode detector that was matched in frequency response to the corresponding multiplier chain, in this case a WR8.0 ZBD (Virginia Diodes, Inc.). The output signal from the detector was processed by two digital lock-in amplifiers (Stanford Research Systems, SR810 and SR830), the first of which was locked to the modulation frequency of the input radiation, and the second of which was locked to the trigger signal from the pulsed valve driver. The output signal intensity was recorded as a function of frequency using a computerized data acquisition routine. The spectral resolution of ≤30 kHz is limited by the frequency point spacing, and spectral linewidths are on the order of 350 kHz. Amplitude modulation was used to measure the relative power from the multiplier across the spectral ranges covered in the experiment, and all spectra were power-normalized before analysis.

A plasma discharge source based on the design of McCarthy and co-workers[37] was used to dissociate methanol. An autoignited plasma was generated between two electrodes in the throat of the expansion during each valve pulse. Teflon spacers were used to separate the first electrode from the valve faceplate by a distance of 2.51 cm. Both electrodes were 0.25 cm thick, and they were separated by a 1 mm thick Teflon spacer. The electrode closest to the valve was made of copper and was held at ground, while a potential of +600 V was applied to the stainless steel outer electrode using a high-voltage power supply (Spelman SL2000). The gas mixture passed through an additional 0.23 cm long channel formed by the Teflon source cap before being expanded into the vacuum chamber. A

dx.doi.org/10.1021/jp3122402 | J. Phys. Chem. A 2013, 117, 9548−9554

discharge current of 27 mA was maintained using a ballast resistance of 10 kΩ in series with the source.

RESULTS AND ANALYSIS

Methanol spectra comparing the signal-to-noise ratio (SNR) of a single-pass optical arrangement and that of the multipass spectrometer are shown in Figure 2. As expected, the 7-fold

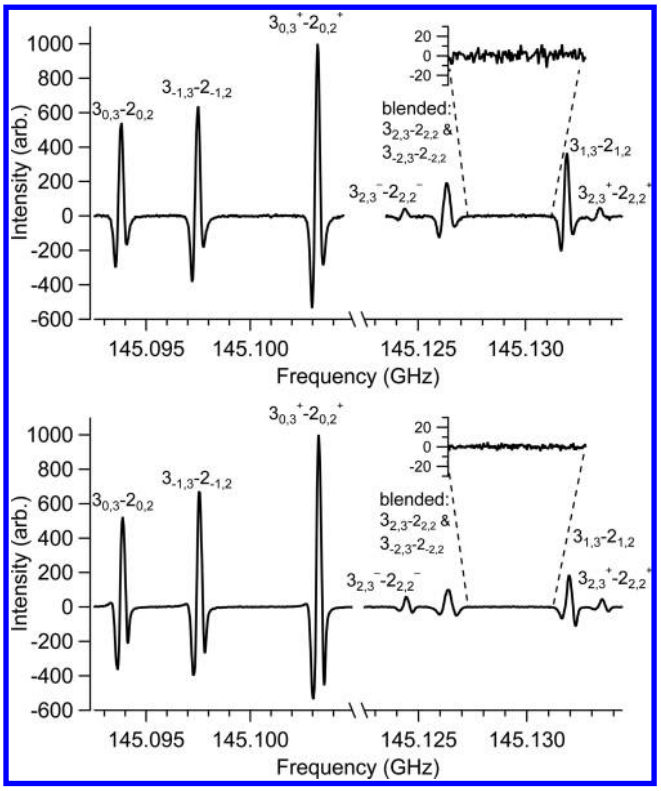

Figure 2. Comparison of methanol spectra using a single pass optical configuration (top) and a multipass optical configuration (bottom). Methanol transitions are labeled with the corresponding quantum numbers. The insets show the noise levels of the baselines in each spectrum.

increase in path length increased the SNR of the spectrum by up to a factor of ∼5; additional increase in SNR was limited by power loss in the probe beam. This power loss was also observed by Schmuttenmaer and co-workers, who worked with a similarly large THz beam size.[12] The relative intensities of the lines in the two spectra indicate that the temperature of the gas probed by the single-pass and multipass setups is similar in value.

The density and temperature of a molecule in a gas sample can be determined using a Boltzmann diagram analysis based on the integrated intensity of the observed spectral lines. In this analysis approach, the integrated intensities of the spectral lines, $\int_{-\infty}^{\infty} I_b d\nu$, and their corresponding upper-state energies, E_u, are related by

$$\int_{-\infty}^{\infty} I_b d\nu = \frac{hc^3 A g_u}{8\pi k \nu^2} \frac{N_T}{Q(T_{rot})} e^{-E_u/kT_{rot}} \quad (2)$$

where h is Planck's constant, k is Boltzmann's constant, c is the speed of light, A is the Einstein A-coefficient for the transition, g_u is the upper state degeneracy, ν is the transition frequency, N_T is the column density, $Q(T_{rot})$ is the rotational partition function, and T_{rot} is the rotational temperature. In an absorption experiment such as the one conducted here, the Einstein A-coefficient used in eq 2 must be converted to the Einstein B-coefficient through the relationship

$$A_{1\rightarrow 0} = B_{1\leftarrow 0} \frac{8\pi h \nu^3}{c^3} \quad (3)$$

and the lower state energies must be used following the relationship $E_u = E_l + h\nu$. Therefore, a plot of $ln[(\int_{-\infty}^{\infty} I_b d\nu)(k/(h^2 \nu B g_u))]$ versus $E_l + h\nu$ gives a line with slope inversely proportional to T_{rot} and with intercept equal to $ln(N_T/Q(T_{rot}))$. A weighted least-squares approach is used for the linear regression analysis, with the uncertainties of the integrated intensities being derived using standard error propagation from the 1σ standard deviation of the noise observed in the power-normalized spectral baseline. The intensity scale for this particular experiment was not calibrated absolutely, precluding quantitative determination of the density. Nonetheless, the integrated intensity of each line is proportional to the product of the peak intensity and the line width at the zero-crossing points for the 2f line shape. Using this approximation, relative abundance ratios can be determined even without absolute intensity calibration by taking the ratio of the intercepts from the Boltzmann diagrams for two species.

It should be noted here that the above derivation neglects any correction for optical depth. Optical depth is a crucial consideration in the determination of absolute densities, and the assumption of optically thin conditions may not be valid in all cases for these types of experiments, especially when extremely low temperatures, broad frequency coverage, and a range of quantum states are considered. However, in this experiment we are not making absolute density determinations, and the impact of optical depth on the slope of the line is negligible. The optical depth correction that would need to be added to the above equations can be neglected in the current work but should be taken into consideration in future applications.

The Boltzmann diagram for methanol determined from the bottom spectrum of Figure 2 is given in Figure 3. The rotational temperature of methanol in the multipass setup as determined from this analysis is 15.1 ± 0.8 K. The strong linear

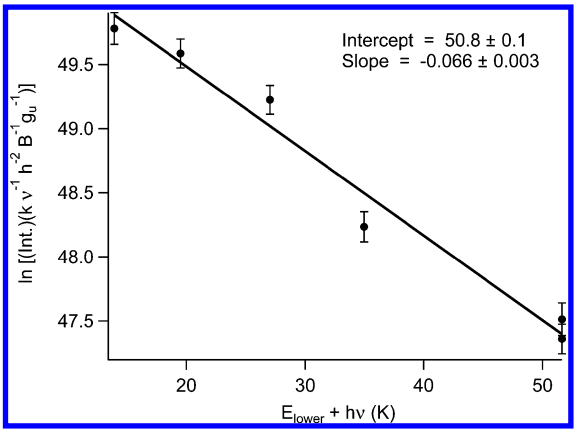

Figure 3. Boltzmann diagram for methanol based on the spectrum from the multipass instrument, shown in the bottom panel of Figure 2, where "Int." is the integrated intensity approximated as the product of the peak intensity and the line width at the zero-crossing points for the 2f line shape.

dx.doi.org/10.1021/jp3122402 | J. Phys. Chem. A 2013, 117, 9548−9554

correlation (R^2 = 0.94) shows that thermodynamic equilibrium is a reasonable approximation for the molecules probed in the expansion. As this experiment is designed to measure the branching fractions of the dissociation products, all product abundances are referenced to the ground vibrational state of methanol. Therefore, the methanol spectrum was reacquired, and the Boltzmann analysis was repeated at a minimum of once per day, ensuring that day-to-day fluctuations in the methanol density were properly accounted for when relative abundances were determined.

In order to test the spectrometer sensitivity and detectability of products, searches were conducted for methanol dissociation products using a high-voltage plasma discharge source. This approach was used in a recent experiment that utilized both laser induced fluorescence and millimeter wave spectroscopy,[38] where the CH_3O and H_2CO products were observed. The CH_3O and H_2CO were similarly observed in the present work as products of methanol dissociation. Sample spectra showing rotational lines of each dissociation product are shown in Figures 4 and 5. In total, 5 lines each of CH_3O and H_2CO were

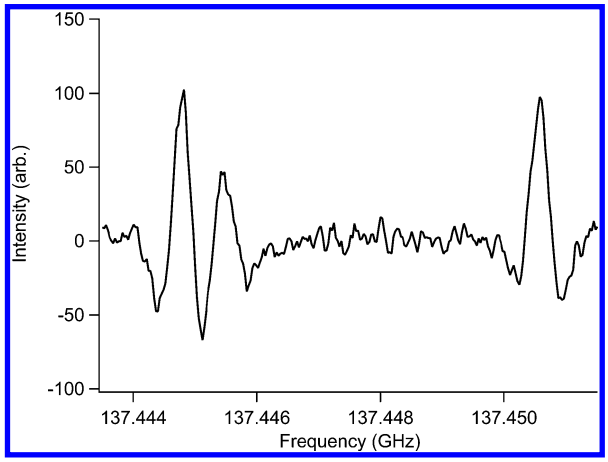

Figure 4. Spectrum of CH_3O detected using a plasma discharge source with a methanol/argon mixture.

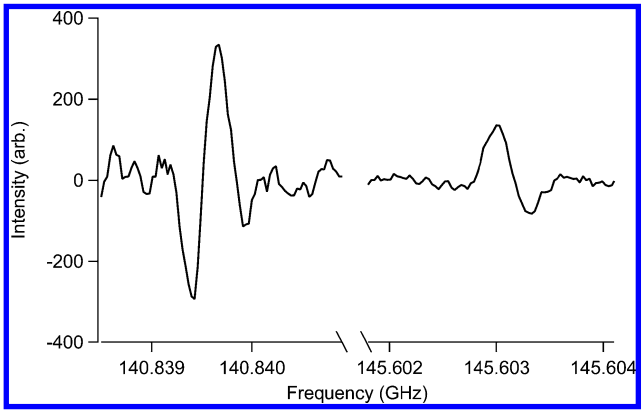

Figure 5. Spectra of H_2CO detected using a plasma discharge source with a methanol/argon mixture.

detected; upper limits were found for two additional lines of CH_3O involving higher energy states. The number of observed lines was limited by the frequency coverage of the multiplier chain that was in use for this particular experiment but provided a sufficient number of transitions to enable a Boltzmann analysis to be performed. Between 20 and 600 spectral scans were averaged for each observed product line in order to increase the signal-to-noise ratio and obtain accurate line intensity information for determination of percent abundance relative to methanol. Additional boxcar averaging across 3 frequency points was used to smooth the spectra for very weak lines. It should be noted that a check of the methanol spectral lines when the discharge source was in use showed no change from the relative intensities or signal-to-noise seen in Figure 2. We conclude from this observation that the spectrometer is probing the expansion in the region where cooling is complete and collisions are minimal.

Relative abundances compared to methanol were determined based on the Boltzmann analysis method described above. The Boltzmann diagrams for the products are shown in Figures 6−8. The CH_3O lines for which upper limits were determined

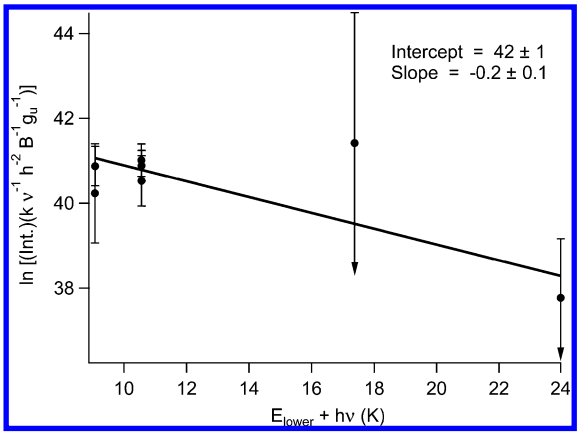

Figure 6. Boltzmann diagram for CH_3O, where "Int." is the integrated intensity approximated as the product of the peak intensity and the line width at the zero-crossing points for the 2f line shape. The two higher energy points that are shown with arrows were the two upper limits; these points are included so that the temperature can be better constrained.

were included in this analysis so that the temperature could be better constrained. The CH_3O product was detected at 0.049 ± 0.05% relative to methanol, and a rotational temperature of 5.4 ± 2.7 K was determined. For H_2CO, only 2 lines were detectable using the double modulation detection scheme locked to the valve pulse. These lines have lower states that are

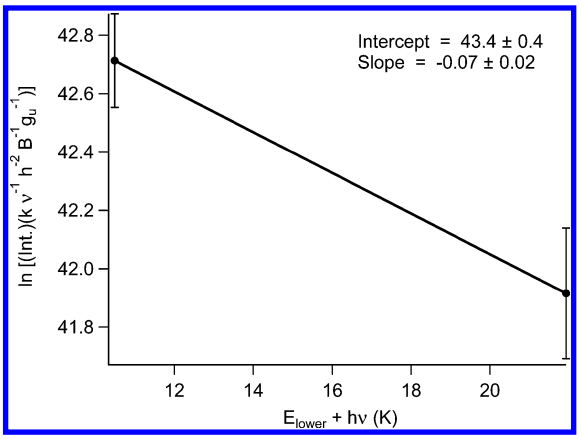

Figure 7. Boltzmann diagram for cold H_2CO, where "Int." is the integrated intensity approximated as the product of the peak intensity and the line width at the zero-crossing points for the 2f line shape.

dx.doi.org/10.1021/jp3122402 | J. Phys. Chem. A 2013, 117, 9548−9554

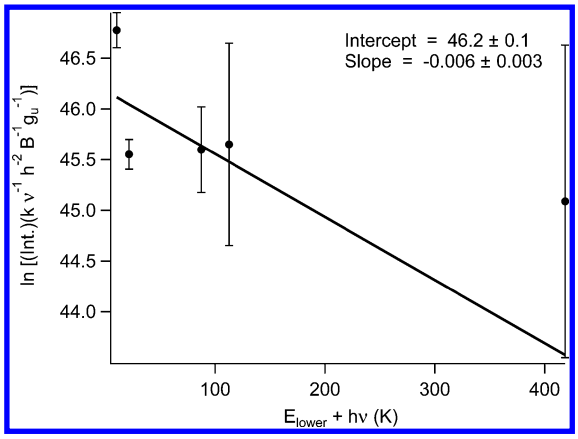

Figure 8. Boltzmann diagram for warm H_2CO, where "Int." is the integrated intensity approximated as the product of the peak intensity and the line width at the zero-crossing points for the 2f line shape.

very low in energy and are therefore expected to be associated with the cold gas in the supersonic expansion. The additional 3 lines were only observed when the second lock-in amplifier was not used, i.e., the detection was not locked to the valve pulse. These lines involve much higher energy states and are presumed to arise from the warmer background gas that is not associated with the expansion. We therefore use the two lines observed for the cold gas to estimate the temperature and abundance relative to methanol. Given that only two lines could be used for this analysis, the rotational temperature and abundance are not very well constrained. Nonetheless, the H_2CO product was detected at 0.036 ± 0.014% relative to methanol in the ground vibrational state, with a rotational temperature of 14 ± 5 K. Analysis of the warm gas component for H_2CO gives an abundance of 8.4 ± 1.5% relative to methanol in the ground vibrational state, with a rotational temperature of 161 ± 80 K. Comparison of these two results for H_2CO indicates that the double-modulation detection scheme is a viable method for probing only the cold gas associated with the expansion and eliminates confusion from any residual background gas in the chamber.

Using the results derived from the cold H_2CO lines, the branching ratio for CH_3O is >1.3 times that for H_2CO in the methanol dissociation mechanism under these conditions; a more quantitative analysis requires detection limits to be determined for the other possible methanol dissociation products (CH_2OH, OH, etc.).

In addition to quantitative information about the dissociation of methanol under these conditions, these results can be used to assess the spectrometer performance. Using the CH_3O spectrum shown in Figure 4, the signal-to-noise ratio of the line at 137.444 GHz is 18. On the basis of the line information in the JPL Molecular Line Catalog and its associated documentation,[39] this spectrum indicates a minimum detectable absorption coefficient of $\alpha_{min} \leq 10^{-9}$ cm $^{-1}$. This value is the extreme limit of sensitivity for this instrument, given the large amount of signal averaging conducted for the methoxy detection. A more reasonable figure of merit based on typical spectrometer performance can be obtained from the methanol spectrum shown in the bottom panel of Figure 2, which yields $\alpha_{min} \approx 5 \times 10^{-9}$ cm $^{-1}$. This is comparable to the α_{min} value obtained with the THz chirped-pulse Fourier Transform technique.[10] It should be noted that the scan rate for the FT instrument is a factor of ∼830 faster than the multipass instrument presented here, making it better suited for broadband spectral studies. Nonetheless, the multipass technique shows great improvement in sensitivity levels compared to standard direct absorption techniques and is therefore widely applicable to reaction dynamics studies involving unstable products.

■ CONCLUSIONS AND FUTURE WORK

This work describes the experimental design and first results from a multipass millimeter/submillimeter spectrometer designed to probe dissociative reaction dynamics. This initial study focused on detection of the CH_3O and H_2CO products from the dissociation of methanol as a proof-of-concept for the experimental design, test of the spectrometer sensitivity limits, and verification of the quantitative nature of the results. The minimum detectable absorption coefficient for this instrument was determined to be $\alpha_{min} \leq 5 \times 10^{-9}$ cm $^{-1}$. Pure rotational spectral lines for methanol dissociation products were monitored via multipass direct absorption spectroscopy. Multiple lines from CH_3O and H_2CO were observed when a plasma discharge was used to dissociate methanol seeded in an argon supersonic expansion. A Boltzmann analysis was performed on the observed spectral lines, and the rotational temperature and abundance relative to methanol were determined for each product. A full quantitative determination of the branching ratios for the methanol dissociation mechanism under these conditions requires detection of the other dissociation products, which is not possible until rotational spectroscopic information on other possible dissociation products such as the CH_2OH radical is obtained.

These results demonstrate the promise that this approach has for examining the dissociation mechanisms for small organic molecules. This study has shown that the unstable products of dissociation reactions can indeed be quantitatively monitored using millimeter/submillimeter spectroscopic techniques at a sensitivity level that enables monitoring of trace species. This method is therefore applicable to the study of any dissociation reaction where the products have permanent dipole moments. This technique also offers a structure-specific detection alternative in cases where mass spectrometry is not a viable option. Therefore, this approach offers a valuable new analytical method for identifying the participants in complicated reaction schemes.

This technique is applicable to a large range of chemical studies, as dissociation reactions involving small organics are of interest in several disciplines, including (but not limited to) astrochemistry, atmospheric chemistry, and combustion chemistry. Such studies are particularly valuable for molecules of astrophysical interest since dissociative reaction dynamics play a fundamental role in interstellar chemistry. Prime targets for astrochemical studies include the photodissociation reactions of small organics, which drive the chemistry on interstellar grain surfaces. Other important astrochemical mechanisms that could be studied using this approach include the formation or dissociative recombination reactions involving organic ions. Beyond dissociation reactions, this technique is more generally applicable to the study of any unstable species that has a permanent dipole moment.

While this technique does have wide-ranging applications, any such study is dependent on the availability of the associated spectral information. In the case of dissociation studies, initial spectral studies that focus on dissociation product identification

dx.doi.org/10.1021/jp3122402 | J. Phys. Chem. A 2013, 117, 9548−9554

and compilation of rotational spectral line catalogs are required before quantitative results can be obtained.

This technique opens the THz window for reaction dynamics studies, as the extension of this instrument to higher frequencies is straightforward, enabling spectroscopic studies across the entire 50 GHz to 1 THz frequency range. Because any direct absorption technique allows for quantification of products, efforts are also underway in our group to incorporate cavity-enhanced spectroscopic techniques into the experiment (DePrince et al., submitted, *Rev. Sci. Instrum.* 2013) so as to increase spectral sensitivity even further beyond what can be achieved with the current multipass spectrometer.

AUTHOR INFORMATION

Corresponding Author

*(S.L.W.W.) E-mail: susanna.widicus.weaver@emory.edu. Phone: +1 (0)404 7274049. Fax: +1 (0)404 7276586.

Notes

The authors declare no competing financial interest.

ACKNOWLEDGMENTS

We thank Michael Heaven for useful discussions regarding these experiments and Michael McCarthy for offering his insights into the use of plasma discharge sources for the study of transient molecules. We thank Emory University for the facilities and staff support that enabled this work. We thank an anonymous reviewer for comments that helped to improve this article. Development of the spectrometer was supported in part by NSF award CHE-1150492. Purchase of the major spectrometer equipment and development of the photolysis sources were supported in part by NASA award NNX11AI07G. All other support came from SLWW's startup funds provided by Emory University.

REFERENCES

(1) Butler, L. J.; Neumark, D. M. *J. Phys. Chem.* **1996**, *100*, 12801−12816.
(2) Garrod, R. T.; Weaver, S. L. W.; Herbst, E. *Astrophys. J.* **2008**, *682*, 283−302.
(3) Dian, B. C.; Brown, G. G.; Douglass, K. O.; Pate, B. H. *Science* **2008**, *320*, 924−928.
(4) Kolbe, W. F.; Leskovar, B. *Rev. Sci. Instrum.* **1985**, *56*, 1577−1581.
(5) Duffy, L. M. *Rev. Sci. Instrum.* **2005**, *76*, 093104.
(6) Lucia, F. C. D. *J. Mol. Spectrosc.* **2010**, *261*, 1−17.
(7) Gopalsami, N.; Raptis, A. C.; Meier, J. *Rev. Sci. Instrum.* **2002**, *73*, 259−262.
(8) Meshkov, A. I.; Lucia, F. C. D. *Rev. Sci. Instrum.* **2005**, *76*, 083103.
(9) Braakman, R.; Blake, G. A. *J. Appl. Phys.* **2011**, *109*, 063102.
(10) Gerecht, E.; Douglass, K. O.; Plusquellic, D. F. *Opt. Express* **2011**, *19*, 8973−8984.
(11) Kaur, D.; de Souza, A. M.; Wanna, J.; Hammad, S. A.; Mercorelli, L.; Perry, D. S. *Appl. Opt.* **1990**, *29*, 119−124.
(12) Schmuttenmaer, C. A.; Cohen, R. C.; Heath, N. P. J. R.; Cooksy, A. L.; Busarow, K. L.; Saykally, R. J. *Science* **1990**, *249*, 897−900.
(13) Xia, W. S.; Zhu, R. S.; Lin, M. C.; Mebel, A. M. *Faraday Discuss.* **2001**, *119*, 191−205.
(14) Ing, W.-C.; Sheng, C. Y.; Bozzelli, J. W. *Fuel Process. Technol.* **2003**, *83*, 111−145.
(15) Chang, A. H. H.; Lin, S. H. *Chem. Phys. Lett.* **2002**, *363*, 175−181.
(16) Chang, A. H. H.; Lin, S. H. *Chem. Phys. Lett.* **2004**, *384*, 229−235.
(17) Endo, Y.; Saito, S.; Hirota, E. *J. Chem. Phys.* **1984**, *81*, 122−135.
(18) Momose, T.; Endo, Y.; Hirota, E.; Shida, T. *J. Chem. Phys.* **1988**, *88*, 5338−5343.
(19) Bocquet, R.; Demaison, J.; Poteau, L.; Liedtke, M.; Belov, S.; Yamada, K.; Winnewisser, G.; Gerke, C.; Gripp, J.; Köhler, T. *J. Mol. Spectrosc.* **1996**, *177*, 154−159.
(20) Brünken, S.; Müller, H. S. P.; Lewen, F.; Winnewisser, G. *Phys. Chem. Chem. Phys.* **2003**, *5*, 1515−1518.
(21) Beaudet, R. A.; Poynter, R. L. *J. Phys. Chem. Ref. Data* **1978**, *7*, 311−363.
(22) Blake, G. A.; Farhoomand, J.; Pickett, H. M. *J. Phys. Chem. Ref. Data* **1986**, *115*, 226−228.
(23) Farhoomand, J.; Blake, G. A.; Pickett, H. M. *Astrophys. J. Lett.* **1985**, *291*, L19−L22.
(24) Brown, J. M.; Zink, L. R.; Jennings, D. A.; Evenson, K. M.; Hinz, A. *Astrophys. J.* **1986**, *307*, 410−413.
(25) Feng, L.; Wei, J.; Reisler, H. *J. Phys. Chem. A* **2004**, *108*, 7903−7908.
(26) Laas, J. C.; Garrod, R. T.; Herbst, E.; Weaver, S. L. W. *Astrophys. J.* **2011**, *728*, 9.
(27) Öberg, K. I.; Garrod, R. T.; van Dishoeck, E. F.; Linnartz, H. *Astron. Astrophys.* **2009**, *504*, 891−913.
(28) Hoch, H.; Patat, F. *Z. Elektrochem.* **1935**, *41*, 494−498.
(29) Fricke, H.; Hart, E. J. *J. Chem. Phys.* **1936**, *4*, 418−422.
(30) Farkas, L.; Hirshberg, Y. *J. Am. Chem. Soc.* **1937**, *59*, 2450−2453.
(31) Porter, R. P.; Noyes, W. A. *J. Am. Chem. Soc.* **1959**, *81*, 2307−2311.
(32) Hagege, J.; Roberge, P. C.; Vermeil, C. *Trans. Faraday Soc.* **1968**, *64*, 3288−3299.
(33) Satyapal, S.; Park, J.; Bersohn, R.; Katz, B. *J. Chem. Phys.* **1989**, *91*, 6873−6879.
(34) Harich, S.; Lin, J. J.; Lee, Y. T.; Yang, X. *J. Chem. Phys.* **1999**, *111*, 5−9.
(35) Harich, S.; Lin, J. J.; Lee, Y. T.; Yang, X. *J. Phys. Chem. A* **1999**, *103*, 10324−10332.
(36) Chen, Z.; Eppink, A. T. J. B.; Jiang, B.; Groenenboom, G. C.; Yang, X.; Parker, D. H. *Phys. Chem. Chem. Phys.* **2011**, *13*, 2350−2355.
(37) McCarthy, M. C.; Chen, W.; Travers, M. J.; Thaddeus, P. *Astrophys. J. Suppl.* **2000**, *129*, 611−623.
(38) Melnik, D. G.; Liu, J.; Chen, M.-W.; Miller, T. A.; Curl, R. F. *J. Chem. Phys.* **2011**, *135*, 094310.
(39) Pickett, H. M.; Poynter, R. L.; Cohen, E. A.; Delitsky, M. L.; Pearson, J. C.; Müller, H. S. P. *J. Quant. Spectrosc. Radiat. Transfer* **1998**, *80*, 883−890.